C. 1

NACA TN 2796

NATIONAL ADVISORY COMMITTEE FOR AERONAUTICS

TECHNICAL NOTE 2796

EXPERIMENTAL STUDY OF THE EFFECTS OF FINITE SURFACE DISTURBANCES AND ANGLE OF ATTACK ON THE LAMINAR BOUNDARY LAYER OF AN NACA 64A010 AIRFOIL WITH AREA SUCTION

By Milton A. Schwartzberg and Albert L. Braslow

Langley Aeronautical Laboratory
Langley Field, Va.

Washington
October 1952

1S

NATIONAL ADVISORY COMMITTEE FOR AERONAUTICS

TECHNICAL NOTE 2796

EXPERIMENTAL STUDY OF THE EFFECTS OF FINITE SURFACE DISTURBANCES AND ANGLE OF ATTACK ON THE LAMINAR BOUNDARY LAYER OF AN NACA 64A010 AIRFOIL WITH AREA SUCTION

By Milton A. Schwartzberg and Albert L. Braslow

SUMMARY

A Langley low-turbulence wind-tunnel investigation was made of an NACA 64A010 airfoil section with continuous suction (area suction) through its porous surfaces to determine its ability to maintain extensive laminar flow behind finite surface disturbances and at angles of attack other than 0°.

Although full-chord laminar flow can be obtained at large values of the Reynolds number through the use of area suction, application of area suction permitted only a small increase in the size of a finite disturbance required to cause premature boundary-layer transition as compared with the nonsuction airfoil. The results indicated that the stability theory for the incompressible laminar boundary layer, which is derived for vanishingly small, two-dimensional, aerodynamically possible disturbances in the boundary layer, is of little practical significance in determining the sensitivity of the laminar boundary layer to surface projections. Combined wake and suction-drag coefficients lower than the drag coefficient of the plain airfoil were obtained through a range of low lift coefficient by the use of area suction.

INTRODUCTION

A two-dimensional experimental and related theoretical investigation of the use of continuous suction (area suction) through porous surfaces on an NACA 64A010 airfoil section has been made (ref. 1) to determine whether area suction sufficiently stabilizes the laminar boundary layer to permit attainment of full-chord laminar flow at large values of the Reynolds number. The investigation of reference 1 indicated that the theoretical concepts regarding area suction are valid and that Reynolds number itself should not be a limiting parameter in attainment of

full-chord laminar flow provided that the airfoil surfaces are maintained sufficiently smooth and fair. The quantitative effects of finite disturbances on the stability of suction-type boundary-layer velocity profiles, however, were not determined in this previous investigation.

The purpose of the present investigation is to provide quantitative information on the stabilizing effect of area suction in the presence of deliberately added two- and three-dimensional surface disturbances. This information is also used to determine whether the laminar-boundary-layer stability theory is valid when small but finite surface irregularities are present. In addition, the previous experiments on a relatively smooth airfoil model (ref. 1) were extended to angles of attack other than 0° to determine whether area suction improved the airfoil drag characteristics at lifting conditions.

The present investigation was conducted at a free-stream Reynolds number of 6×10^6, except for an initial series of drag measurements through a range of Reynolds number which served as a basis for comparison of the present surface condition of the model with that during the previous investigations. Measurements that were made included wake drags, suction-flow quantities, suction-air pressure losses, boundary-layer velocity profiles, and stethoscopic indications of the position of transition from laminar to turbulent flow.

SYMBOLS

α	section angle of attack
c	airfoil chord
b	span of porous surface
x	distance along chord from leading edge of airfoil
s	distance along surface from leading edge of airfoil
y	distance normal to surface of airfoil
ρ_o	free-stream mass density
U_o	free-stream velocity
q_o	free-stream dynamic pressure, $\frac{1}{2}\rho_o U_o^2$

H_o	free-stream total pressure
p	local static pressure on airfoil surface
U	local velocity parallel to surface at outer edge of boundary layer
S	airfoil pressure coefficient, $\frac{H_o - p}{q_o}$ or $\left(\frac{U}{U_o}\right)^2$
u	local velocity parallel to surface and inside boundary layer
ν	kinematic viscosity
R	free-stream Reynolds number based on airfoil chord, $U_o c/\nu$
Q	total volume rate of flow through both airfoil surfaces
C_Q	suction-flow coefficient, Q/bcU_o
H_i	total pressure in model interior
C_p	suction-air pressure-loss coefficient, $(H_o - H_i)/q_o$
c_{d_w}	section wake-drag coefficient
c_{d_s}	section suction-drag coefficient, $C_Q C_p$
c_{d_T}	section total-drag coefficient, $c_{d_s} + c_{d_w}$
μ	absolute viscosity
t	thickness of porous material
v_o	velocity through airfoil surface (for suction, $v_o < 0$)
Δp	static pressure drop across porous surface
c_{v_o}	porosity factor, $\left\|\frac{v_o}{\Delta p}\right\| \mu t$, length^2
d	chordwise extent of roughness projection

k height of roughness projection normal to surface of airfoil

u_k local velocity inside boundary layer at a distance k from the surface

R_k projection Reynolds number, based on projection height and velocity in boundary layer at a distance k from the surface, ku_k/ν

$R_{k_{cr}}$ value of R_k for which an abrupt forward movement of transition occurs

δ^* displacement thickness of the boundary layer, $\int_0^\infty \left(1 - \frac{u}{U}\right)dy$

θ momentum thickness of the boundary layer, $\int_0^\infty \frac{u}{U}\left(1 - \frac{u}{U}\right)dy$

$R\delta^*$ boundary-layer Reynolds number, $U\delta^*/\nu$

$\left(R\delta^*\right)_{cr}$ value of $R\delta^*$ at which disturbance is neither damped nor amplified

MODEL DESCRIPTION

The model tested was the same 3-foot-chord, two-dimensional NACA 64A010 airfoil model of reference 1 with new sintered-bronze surfaces of a porosity equal to that of the surfaces used for configuration 3 of reference 1 $\left(c_{v_o} = 0.0525 \times 10^{-10} \text{feet}^2\right)$. The airfoil ordinates are presented in reference 2. The theoretical pressure-coefficient distribution of this airfoil at 0° angle of attack, when mounted in the Langley low-turbulence pressure tunnel (not the free-air pressure distribution), is presented in figure 1.

The sintered-bronze skin occupied the center 12 inches of the 36-inch span of the model on both the upper and lower surfaces. The leading edge of the model was formed by a sheet of duralumin butted to the bronze. Both surfaces were glazed and faired with hard-drying putty from the leading edge to the 5-percent-chord station, so that the suction was applied from this station to the trailing edge.

The internal model structure corresponded to the uncompartmented configurations described in reference 1 and shown in figure 2; consequently, the model internal pressure was substantially uniform.

An indication of the smooth surface condition of the model is provided by the waviness measurements of the sintered-bronze skin taken both chordwise and spanwise and presented in figures 3 and 4. The waviness measurements present relative rather than absolute variations from the true airfoil profile. The degree of waviness of the bronze surfaces can be estimated by comparison with the measurements on the cast-aluminum end sections where the profiles varied by no more than ±0.003 inch from the true airfoil profile.

APPARATUS AND TESTS

The model was tested at a Mach number of approximately 0.3 in the Langley low-turbulence pressure tunnel described in reference 3. Wake drags, suction-flow quantities, suction-air pressure losses, and boundary-layer velocity profiles were measured as described in reference 1. The region of boundary-layer transition, both on the smooth model and behind the roughness elements, was determined aurally by means of a stethoscope attached to a 0.003-inch-internal-diameter total-pressure tube mounted at the end of a rigid rod which was inserted into the boundary layer and moved manually. Movement of the total-pressure tube on the surface of the solid end sections of the model from the region of favorable pressure gradient where the flow was laminar to the region of adverse pressure gradient where the flow was turbulent revealed a very obvious distinction in sound between the laminar and turbulent flow. After the observer's ear had been "calibrated," it was a simple matter to differentiate between a laminar and turbulent boundary layer on the porous surfaces.

Boundary-layer velocity profiles were determined from measurements of the total pressures through the boundary layer and the local static pressure with a group of nine total-pressure tubes and one static-pressure tube. Four of the total-pressure tubes, which differed in external and internal diameter, were placed in contact with the airfoil surface to permit the measurement of the total pressures close to the surface. Reference 4 presents a correction that must be applied to the measurements of tube heights for total-pressure tubes in contact with the surface. This correction, which was determined from measurements on an airfoil without boundary-layer suction, was applied to the measurements made on the present model which had inflow through the surfaces. This surface inflow probably has an important influence on the effective height of the total-pressure tubes. Inasmuch as the tubes in contact with the model were located in the steepest portion of the boundary-layer velocity gradient, small errors in the measurement of and corrections to the tube heights result in large errors in the measurement of the velocity gradients near the model surface.

Roughness effects were simulated at two chordwise stations on the upper surface of the model: 0.30c in the region of the favorable pressure gradient and 0.75c in the region of the adverse pressure gradient. The two-dimensional roughness elements consisted of tape strips of various heights which spanned the bronze portion of the model. The three-dimensional roughness element was a smooth, headless, cylindrical nail of 0.024-inch diameter driven into the bronze surface to various projection heights.

Frequent vacuum cleaning and light sanding of the bronze skin was performed in an effort to maintain the model pores dust-free and the surface imperfections at a minimum. No measurable change in the porosity of the bronze skin occurred during the course of the investigation. Wake drags were measured periodically in order to check the condition of the model surface.

RESULTS AND DISCUSSION

Investigation of Model Without Deliberately Added Roughness

Before any surface irregularities were added to the present model, wake-drag measurements and stethoscopic indications of the location of transition on the smooth model were obtained to provide a comparison of the present porous surfaces with those of configuration 3 of reference 1 and to provide a basis for determining the effect of the deliberately added surface disturbances.

After an initial series of spanwise surveys of section wake-drag coefficient (fig. 5), all further measurements were obtained within a 2-inch region about the model center line where the flow is believed to be unaffected by any disturbances originating at the chordwise junctures between the sintered-bronze skin and the solid end sections of the model. In general, figure 5 indicates that the right side of the model was somewhat less smooth than the left, an indication that was confirmed a number of times during the tests.

Wake-drag measurements through a range of suction-flow coefficient C_Q were made at three values of the Reynolds number at an angle of attack of 0° (fig. 6). Fairly good agreement with the results for configuration 3, reference 1, was obtained at Reynolds numbers from 6×10^6 to 15×10^6. At a Reynolds number of 20×10^6, however, the minimum section wake-drag coefficient was greater than that of reference 1 and the drag rise with decreasing suction-flow coefficient occurred at a higher value of C_Q. These differences may be attributed to a greater degree of surface waviness of the present model. Although

surface waviness surveys were not made for the model of reference 1, it is believed on the basis of visual observations that the present model surface was more wavy. Quantitative information on the effects of surface waviness on the stability of the suction-type laminar boundary layer was not obtained in this investigation, but a comparison of the results of the present investigation with the results for configuration 3 of reference 1 (fig. 6) does indicate that improved surface fairness over that shown in figures 3 and 4 might have avoided a forward movement of transition with an increase in Reynolds number.

The sudden rise in drag coefficient with an increase in suction-flow coefficient above a value of 0.0016 at the Reynolds number of 20×10^6 (fig. 6) is probably caused by the increase in size of the imperfections in the sintered-bronze surface relative to the boundary-layer thickness at the large values of suction-flow coefficient and Reynolds number. Because of the sensitivity of the laminar boundary layer at large values of the Reynolds number to imperfections inherent in the bronze skin, all the tests with deliberately added roughness were made at a free-stream Reynolds number of 6×10^6 so that the effect of the inherent skin irregularities was negligible through the range of suction-flow coefficients investigated.

The variation of the position of transition of the boundary layer from laminar to turbulent flow with suction-flow coefficient at a Reynolds number of 6×10^6 is presented in figure 7 for the model upper surface devoid of any deliberately added roughness elements. These results are the basis for the determination of the effect of the deliberately added surface disturbances. The trend of the data of figure 7, which were obtained by the use of the stethoscope, is consistent with the variation of section wake-drag coefficient at the same Reynolds number (fig. 6); that is, a gradual rearward movement of the position of transition with an increase in suction-flow coefficient occurs simultaneously with a gradual reduction in drag coefficient, and the value of C_Q at which the minimum value of drag coefficient is reached coincides with the suction-flow coefficient required for full-chord laminar flow.

In order to calculate the parameters involved in an analysis of the results obtained with the deliberately added surface projections, knowledge is required of the boundary-layer profile on the smooth model at the position at which the projection is to be added.

The boundary-layer velocity profiles measured on the smooth airfoil at the 0.75c station for several values of suction-flow coefficient are shown in figure 8. It is of interest to note that the value of C_Q at which turbulent flow occurs at 0.75c, as indicated by the velocity

profiles (C_Q = 0.00079 and 0.00076), agrees very well with the value of C_Q for transition at the same station as indicated by the stethoscope (fig. 7).

The boundary layer at the 30-percent-chord station was too thin for reliable measurement. The velocity profiles at 0.30c, therefore, were calculated by the approximate method of reference 5 through the use of calculated chordwise inflow-velocity distributions and are presented in figure 9. The inflow-velocity distributions were calculated from the airfoil external pressure coefficients (fig. 1) and the measured suction-air pressure-loss coefficients C_p by means of the following relation from appendix A of reference 1:

$$-\frac{v_o}{U_o} = \frac{c_{v_o}}{2ct} R(C_p - S) \qquad (1)$$

Values of C_Q obtained from integrations of these estimated chordwise inflow-velocity distributions agreed very closely with the measured values of suction-flow coefficient as shown in the following table:

Measured C_Q	Estimated C_Q
0.00310	0.00317
.00117	.00110

Effects of Finite Surface Disturbances

An investigation of the quantitative effects of two-dimensional tape strips and three-dimensional cylindrical projections on the chordwise position of boundary-layer transition from laminar to turbulent flow on an airfoil without boundary-layer control is reported in reference 6. The results indicated that, with projections present, transition occurred either at the usual position found without surface projections or at a position close behind the roughness elements. Whether transition occurred at the one place or the other was found to be a function of the projection fineness ratio d/k and the value of a Reynolds number R_k based on the projection height and the velocity in the boundary layer at the top of the projection as measured without the projection present. An experimental correlation of the value of the projection Reynolds number required to cause transition close behind the projection $R_{k_{cr}}$ and the projection fineness ratio is given in reference 6.

The present tests were made to determine whether any increase in the size of the roughness, over that found to cause transition on an airfoil without suction, could be tolerated with area suction applied at the airfoil surfaces. Any increase in the permissible size of the roughness would be evidenced by a corresponding increase in the value of $R_{k_{cr}}$. A comparison of the values of $R_{k_{cr}}$ obtained in the present investigation with those presented in reference 6, therefore, is used as a basis for determining whether the use of continuous suction permits an increase in the size of tolerable roughness. In order to facilitate a direct comparison with the results of reference 6, two-dimensional tape strips and three-dimensional cylindrical projections were used in the present investigation.

The projection Reynolds number R_k which was varied by changes in the projection height and in the suction quantity was calculated from the measured quantities by means of the following relation:

$$R_k = \frac{u_k k}{\nu} = \frac{u_k}{U} \frac{U}{U_o} \frac{k}{c} R \qquad (2)$$

Three-dimensional roughness elements.- Figure 10 shows the extent of laminar flow behind a nail of 0.024-inch diameter and various projection heights located 1 inch left of the model center line at the 0.75c station. The values of C_Q at which premature boundary-layer transition occurred because of the presence of the nail were determined from the stethoscopic findings.

A nail height of 0.052 inch which extended well into the boundary layer was found to cause transition immediately behind the nail at all values of C_Q. This same condition prevailed for all decreased values of the nail height tested down to and including a nail height of 0.015 inch. For a value of the nail height of 0.012 inch, laminar flow extended behind the nail to a chordwise position that was the same as the location of transition for the airfoil without the roughness element for values of C_Q up to 0.00135, a result which indicated that the nail was not causing premature transition at these values of C_Q. An increase in suction flow coefficient from 0.00135 to 0.00149 was found to cause a large forward movement of the position of transition from 0.975c to 0.785c. Further increases in the suction quantity advanced transition to a position very close behind the nail.

Full-chord laminar flow existed at a value of C_Q of 0.0016 for a nail height of 0.010 inch. A small increase in suction-flow coefficient, however, produced bursts of turbulence in the boundary layer between

0.85c and the trailing edge. A further increase in suction-flow coefficient to 0.00182 produced an unsteady roaring between 80 and 85 percent chord with fully developed turbulent flow from 85 percent chord to the trailing edge. Higher values of C_Q moved transition close behind the nail.

A nail height of 0.008 inch permitted laminar flow to extend to the model trailing edge through a large range of C_Q up to the maximum obtainable with the available blower system. At a value of C_Q of 0.00307, bursts of turbulence were heard in the boundary layer in the region from 0.78c to the trailing edge. In all probability, a further increase in suction would have instituted fully developed turbulent flow behind the nail. Inasmuch as the highest available suction-flow coefficient was insufficient to attain a critical projection Reynolds number with a nail height of 0.008 inch, full-chord laminar flow probably would have existed up to the maximum test value of C_Q for further decreased values of the nail height.

Inasmuch as the movement of transition from a downstream position on the airfoil to a position close behind the disturbance takes place through a range of suction-flow coefficient, and, therefore, of R_k, selection of the critical value of R_k may appear difficult. Figure 11, however, computed by means of equation (2) and the boundary-layer-velocity profiles of figure 8, shows that the change in R_k corresponding to the change in C_Q required to move the transition point from its downstream position to the region of the disturbing element is slight, so that any inaccuracy in the measurement of $R_{k_{cr}}$ associated with uncertainty in the determination of the critical suction-flow coefficient is small.

Figure 12(a) depicts the extent of laminar flow behind a nail of 0.024-inch diameter located on the model center line at the 0.30c station for two values of the projection height through the available range of suction-flow coefficient. Tested values of the projection height of 0.007 inch and greater produced immediate transition regardless of the suction-flow coefficient.

A nail height of 0.0055 inch was found to permit continuation of laminar flow behind the nail for values of C_Q up to 0.00126. At this value of C_Q turbulent bursts were heard behind the nail extending from the 0.30c station to the 0.80c station behind which the flow was fully turbulent. The flow was fully turbulent from close behind the nail to the trailing edge at a value of C_Q of 0.00139 and for all higher values.

A nail height of 0.0045 inch did not alter the extent of laminar flow over the airfoil below a suction-flow coefficient of 0.00261. At

this value of C_Q, scattered bursts of turbulence were heard behind the nail to the 40-percent-chord station beyond which they were no longer detected and the flow remained laminar to the trailing edge. A suction-flow coefficient of 0.00282 produced the characteristic roaring sounds of turbulence interspersed with bursts behind the nail to the 0.45c station. In this case, the bursts heard with the stethoscope can be interpreted as an occasional return to the laminar condition of the flow behind the projection which was primarily turbulent. Between the 0.45c station and the 0.50c station, the roaring was eliminated and replaced by light bursts of turbulence. From the 0.50c station to the trailing edge, all signs of turbulence had disappeared and laminar flow was found to extend all the way to the trailing edge. At a suction-flow coefficient of 0.00310, fully turbulent flow existed behind the nail to the 42-percent-chord station. Between this station and the 51-percent-chord station, fully turbulent flow was no longer detected and only bursts of turbulence were heard. From the 0.51c station to the trailing edge, undisturbed laminar flow existed. These indications of the return of a turbulent flow to the laminar condition are believed to be the first experience of this type to be reported in the literature. It should be noted that these phenomena were observed only in the wake of a single cylindrical projection situated in the region of favorable pressure gradient at high suction-flow coefficients and when the flow about the roughness element was such that probably only slight increases in C_Q or R_k would be required to establish complete turbulence from the projection to the airfoil trailing edge. A nail height of 0.003 inch was found to permit continuation of laminar flow behind the nail to the trailing edge within the range of suction-flow coefficients available.

Although a specific choice of a critical value of C_Q may again seem difficult to make on the basis of these data, it is found (fig. 13) that the variation of R_k with C_Q is so slight as to make a specific choice of a critical C_Q relatively unimportant. The assumption has been made that only a relatively small increase of C_Q beyond the maximum test value of 0.0031 would be required to produce fully turbulent flow behind the nail of 0.0045-inch height. The airfoil wake-drag coefficient with a nail of 0.0055-inch height at the 30-percent-chord station increased substantially with the large forward movement of transition on the model upper surface and permits evaluation of the critical projection Reynolds number on this basis. These drag measurements are shown in figure 12(b) and they are seen to be in close agreement with the observations made by means of the stethoscope.

Two-dimensional roughness elements.- Two-dimensional roughness elements were simulated by tape strips of 0.250-inch width glued to the

model surface across the span at the two chordwise test stations. At the 75-percent-chord station, a tape strip of 0.0095-inch height produced transition at or near the strip at all test values of C_Q. A tape strip of 0.008-inch height permitted laminar flow no farther back than the 0.82c station at any value of C_Q. Laminar flow to the trailing edge at some spanwise stations existed at a value of C_Q of 0.00112 with a strip of 0.005-inch height. This condition corresponds to a value of R_k of 139 for a fineness ratio d/k equal to 50. Increases in the value of C_Q, however, moved the position of transition progressively forward on the airfoil to the strip so that a critical Reynolds number could not be established. A value of R_k of 269 for this fineness ratio caused immediate transition at the strip. A tape strip of 0.0035-inch height permitted laminar flow to the trailing edge up to the maximum available C_Q. This indicates a value of $R_{k_{cr}}$ greater than 149 for a value of d/k of 71.4.

At the 30-percent-chord line, a two-dimensional strip of 0.005-inch height permitted laminar flow to only the 0.50c station at a value of C_Q of 0.00087. Higher suction quantities again moved the transition position gradually forward on the airfoil to the neighborhood of the strip. A possible range of $R_{k_{cr}}$ from values of 320 to 440 is indicated by the data. Increased strip heights caused immediate transition at the strip throughout the range of suction quantity available. A tape strip of 0.0035-inch height did not change the extent of laminar flow from that which existed on the model without the roughness elements. At a suction-flow coefficient of 0.00310, the value of R_k for this strip height is 398 for a value of d/k of 71.4. The critical value of R_k is then greater than 398.

Comparison with results for nonporous airfoil.- Most of the results obtained with the finite two-dimensional roughness elements can be interpreted as lying within the range of scatter of the data similarly obtained on surfaces without suction as presented in figure 15 of reference 6. The value of $R_{k_{cr}}$ greater than 398 for $\frac{d}{k} = 71.4$ obtained at 0.30c for the tape strip of 0.0035-inch height is the only point suggesting any notable increase in $R_{k_{cr}}$ due to suction with two-dimensional finite disturbances present. The values of $R_{k_{cr}}$ obtained for two-dimensional roughness elements on the airfoil with suction are comparable to those obtained for the airfoil without suction since the 0.250-inch-wide strips used in the present tests extended over a chordwise region of the airfoil d/c that corresponds closely to that covered by the strips of reference 6. Other strip widths would require a correlation involving the additional parameter d/c to account for the blanketed chordwise region that is not subject to suction.

For three-dimensional disturbances the variation of the square root of the critical projection Reynolds number with projection fineness ratio for airfoils without boundary-layer control is presented in figure 14 as obtained from the faired curve of figure 12 of reference 6. Also presented in the same figure for comparison are the results obtained in the present investigation with three-dimensional projections and continuous suction. Although the data are sparse, the indicated trend of $\sqrt{R_{k_{cr}}}$ with d/k is of the same type as that of reference 6.

Application of area suction increased the critical projection Reynolds number over that measured without boundary-layer control only by a factor of approximately 2. This increase in $R_{k_{cr}}$ corresponds to an increase in permissible height of the projection of less than 40 percent for a given value of the boundary-layer thickness. At a given chordwise position, however, the boundary layer would be thinner with area suction than without area suction so that the increase in allowable projection height would be even smaller.

The stability theory for the incompressible laminar boundary layer indicates that the stability of boundary-layer velocity profiles obtained with area suction when only vanishingly small, two-dimensional, aerodynamically possible disturbances are present in the boundary layer is much greater than that of nonsuction profiles. The experimental results just presented indicate that area suction as applied in the present investigation resulted in only a small increase in the allowable size of small but finite surface irregularities. This result suggests very strongly that the small-disturbance, laminar-boundary-layer stability theory is inapplicable where small but finite surface irregularities are present. The applicability of this theory can be judged more precisely, however, on the basis of a comparison of the values of $R\delta^*$ at which transition was found to occur in the presence of finite surface disturbances and the theoretical values of $(R\delta^*)_{cr}$ calculated for the boundary-layer velocity profiles obtained on the model.

Determination of the value of $(R\delta^*)_{cr}$ for a given boundary-layer velocity profile, on the basis of the laminar-boundary-layer stability theory, requires an accurate knowledge of the second derivative of the velocity profile. The data points of figure 8, through which the velocity profiles have been faired, are not sufficiently accurate to permit a precise determination of the second derivatives of the profiles. Values of boundary-layer thickness, such as θ and δ^*, however, depend upon an integration of the faired velocity profiles and, therefore, can be determined with a satisfactory degree of accuracy.

Measured values of θ, chord Reynolds number, and local airfoil pressure gradient can be employed in the Schlichting method of defining suction velocity profiles (ref. 5) to determine the local inflow velocity that would be required under the specified measured conditions to obtain the asymptotic suction profile. The critical boundary-layer Reynolds number predicted by the laminar boundary-layer stability theory for the asymptotic profile is of the order of 40,000. Through the range of suction-flow coefficient in which critical values of R_k were measured, the actual local inflow velocities were found to be greater than the local inflow velocities required for the asymptotic suction profile as shown in the following table:

Measured C_Q	Calculated C_Q $\oint \frac{v_o}{U_o} d\frac{s}{c}$; v_o/U_o from equation (1)	Value of $-v_o/U_o$ at 0.75c from equation (1)	Value of $-v_o/U_o$ at 0.75c required for asymptotic suction profile
0.00310	0.00317	0.00170	0.00082
.00172	.00169	.00092	.00059
.00141	.00136	.00076	.00055

The values of $(R\delta^*)_{cr}$, therefore, for the experimental velocity profiles were apparently of the order of magnitude of the value for the asymptotic shape. This conclusion is further verified by figure 15 where data points for the measured velocity profiles of figure 8 agree very closely with the asymptotic suction profile except for the experimentally inaccurate values close to the airfoil surface. The boundary-layer Reynolds numbers for which transition occurred immediately behind the finite surface irregularities varied from approximately 1500 to 3000. Inasmuch as these experimental values of $(R\delta^*)_{cr}$ are so much smaller than the theoretical value of $(R\delta^*)_{cr}$, the significance of $(R\delta^*)_{cr}$ as calculated by the small-disturbance, laminar-boundary-layer stability theory is evidently very different from that of the experimentally determined minimum critical Reynolds number for laminar flow in a pipe. In the latter case, if the Reynolds number of the flow, based on the pipe diameter, is less than about 2000, the flow will return to the laminar state regardless of the magnitude or nature of any disturbance introduced into the flow.

The nature of the surface irregularities to which the boundary layers of the present investigation and those of reference 1 were subjected may be classified into two types: (a) those having a minimum radius of curvature much larger than the boundary-layer thickness, that is, surface

waviness, and (b) those having a minimum radius of curvature of the order of or less than the boundary-layer thickness, that is, surface projections. In the former case, the theory of small disturbances may well be applicable as the effect of the irregularities could be calculated through their known effect on the pressure distribution. In the latter case, however, the theory of small disturbances appears to be of little practical value in determining the sensitivity of the laminar boundary layer to such surface irregularities.

An evaluation of boundary-layer-control effectiveness in the maintenance of extensive laminar boundary layers can be attempted on the basis of this investigation and that of reference 1 as well as other investigations employing a number of discrete suction slots (for example, ref. 7). The application of continuous suction resulted in only a slight stabilization of the boundary layer on an airfoil with small but finite surface irregularities. The investigations of multiple suction slots indicated that the difficulty involved in the maintenance of extensive laminar boundary layers on airfoils incorporating such a system would be at least as great as that encountered in the past in the maintenance of extensive laminar layers on low-drag airfoil sections without boundary-layer control. Both methods of boundary-layer control offer the possibility of maintaining extensive laminar flow at large values of the Reynolds number, but each method requires the maintenance of extremely smooth airfoil surfaces.

Effect of Angle of Attack

The final group of tests in the present investigation was made on the smooth model through an angle-of-attack range from -3° to 6° to determine whether area suction provided an extension of the low-drag range. The airfoil wake- and total-drag coefficients obtained with suction through the angle-of-attack range for values of C_Q of 0.0010, 0.0016, and 0.0020 are presented in figure 16. The suction-drag coefficients c_{d_s} which have been added to the wake-drag coefficients to obtain the total-drag coefficients were based on the minimum values of airfoil suction-air pressure-loss coefficient C_p necessary to prevent outflow at each of the different angles of attack. These values of C_p are included in figure 16. For this particular model, which is not subject to outflow in the low-pressure region over the nonporous leading 5 percent of the model surface, the minimum permissible value of C_p assumed for each angle of attack is that corresponding to the maximum value of the airfoil pressure coefficient over the porous surfaces. The airfoil pressure-coefficient distribution existing at each angle of attack was calculated by the method outlined in reference 8.

The results presented show a decrease in the total drag of the airfoil with suction as compared with that of the airfoil without suction through a range of angle of attack from -3° to 2°. The unsymmetrical nature of the results emphasizes the differences in surface condition existing between the upper and lower surfaces of the model. The higher values of wake-drag coefficient measured at 0° angle of attack in this series of tests as compared with the earlier measurements shown in figure 6 are a further indication of the sensitivity of the porous surface. If the original model condition had been maintained, a general lowering of the drag coefficients would have been achieved. It is also conceivable that improved surface conditions would have resulted in lower total-drag coefficients over a wider range of angle of attack of the airfoil. This observation is based on a comparison of the results obtained at positive and negative angles of attack.

This decrease in the total-drag coefficient of the airfoil at lifting conditions will enhance the lift-drag-ratio characteristics of the airfoil in the range of low lift coefficients if the surfaces are maintained sufficiently smooth. The indications, however, are unfavorable to the application of area suction at higher lift coefficients where figure 16 shows an increase in the total-drag coefficient of the airfoil with suction over that of the airfoil without suction.

CONCLUSIONS

A Langley low-turbulence wind-tunnel investigation of an NACA 64A010 airfoil section with porous surfaces was made to determine the effectiveness of continuous suction in maintaining full-chord laminar flow behind finite disturbances and at angles of attack other than 0°. The results of this investigation indicate the following conclusions:

1. The use of area suction resulted in a relatively small increase in the size of a small but finite surface disturbance required to cause premature boundary-layer transition as compared with that for the airfoil without suction. With or without continuous suction, the maximum size of a protuberance that will not cause premature transition is small with respect to the boundary-layer thickness.

2. The laminar-boundary-layer stability theory, which is based on vanishingly small, two-dimensional, aerodynamically possible disturbances in the boundary layer, appears to be of little practical significance in determining the sensitivity of the laminar boundary layer to surface projections.

3. By the use of area suction it was possible to restore the flow in the boundary layer from the turbulent to the laminar state in the wake of

a single cylindrical projection situated on the airfoil in the region of favorable pressure gradient at high suction-flow coefficients. The flow about the projection, however, was such that probably only slight increases in suction quantity or projection Reynolds number would have been required to establish complete turbulence from the projection to the airfoil trailing edge.

4. Combined wake and suction drag coefficients lower than the drag coefficient of the plain airfoil can be obtained through a range of low lift coefficient by the use of area suction, provided that the airfoil surfaces are maintained sufficiently smooth.

Langley Aeronautical Laboratory,
National Advisory Committee for Aeronautics,
Langley Field, Va., July 7, 1952.

REFERENCES

1. Braslow, Albert L., Burrows, Dale L., Tetervin, Neal, and Visconti, Fioravante: Experimental and Theoretical Studies of Area Suction for the Control of the Laminar Boundary Layer on an NACA 64A010 Airfoil. NACA Rep. 1025, 1951. (Supersedes NACA TN 1905 by Burrows, Braslow, and Tetervin and NACA TN 2112 by Braslow and Visconti.)

2. Loftin, Laurence K., Jr.: Theoretical and Experimental Data for a Number of NACA 6A-Series Airfoil Sections. NACA Rep. 903, 1948. (Supersedes NACA TN 1368.)

3. Von Doenhoff, Albert E., and Abbott, Frank T., Jr.: The Langley Two-Dimensional Low-Turbulence Pressure Tunnel. NACA TN 1283, 1947.

4. Von Doenhoff, Albert E.: Investigation of the Boundary Layer About a Symmetrical Airfoil in a Wind Tunnel of Low Turbulence. NACA ACR, Aug. 1940.

5. Schlichting, H.: An Approximate Method for Calculation of the Laminar Boundary Layer With Suction for Bodies of Arbitrary Shape. NACA TM 1216, 1949.

6. Loftin, Laurence K., Jr.: Effects of Specific Types of Surface Roughness on Boundary-Layer Transition. NACA ACR L5J29a, 1946.

7. Burrows, Dale L., and Schwartzberg, Milton A.: Experimental Investigation of an NACA 64A010 Airfoil Section With 41 Suction Slots on Each Surface for Control of Laminar Boundary Layer. NACA TN 2644, 1952.

8. Abbott, Ira H., Von Doenhoff, Albert E., and Stivers, Louis S., Jr.: Summary of Airfoil Data. NACA Rep. 824, 1945. (Supersedes NACA ACR L5C05.)

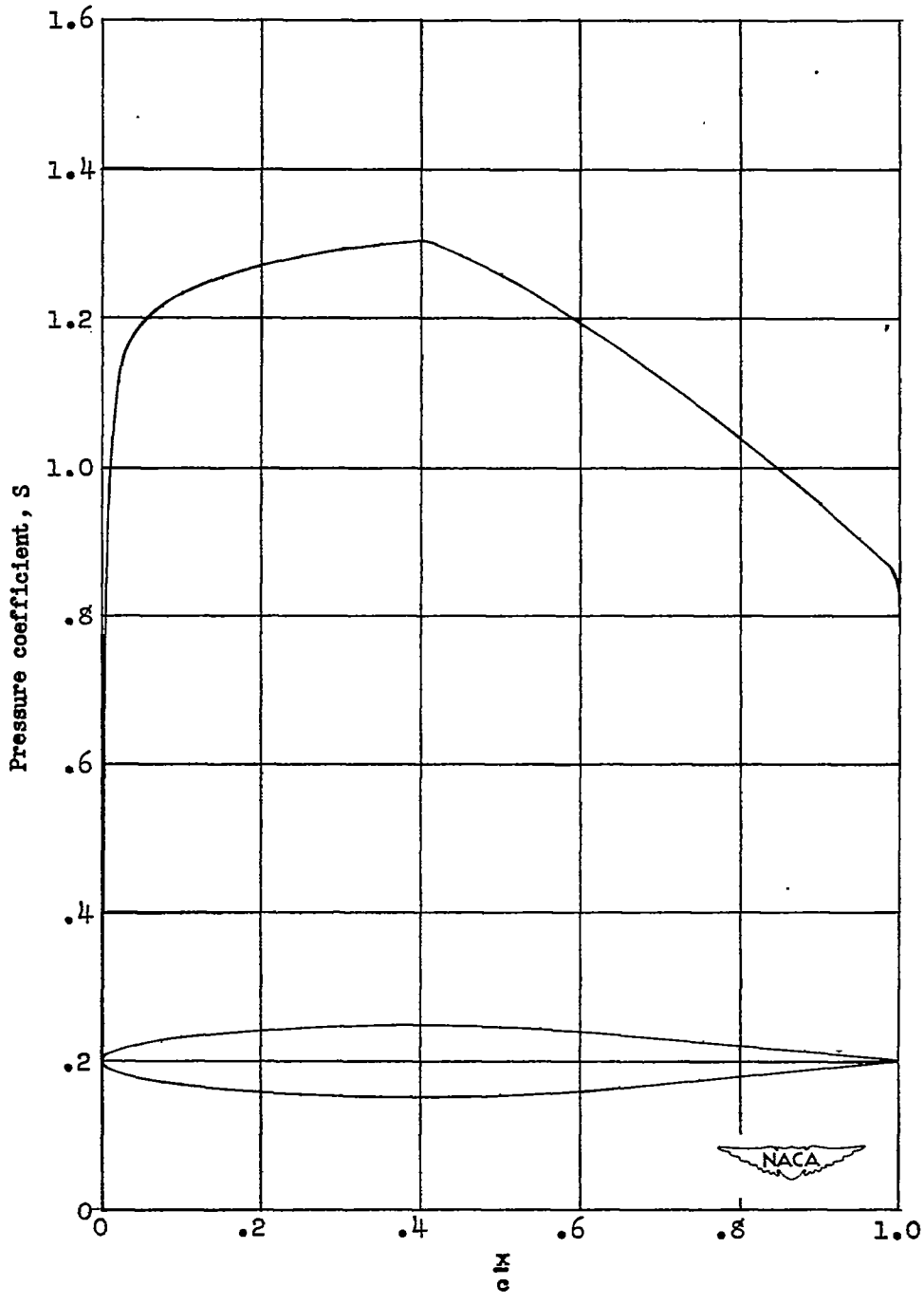

Figure 1.- Theoretical pressure-coefficient distribution on the NACA 64A010 airfoil when mounted in the Langley low-turbulence pressure tunnel (not the free-air pressure distribution). $\alpha = 0^{\circ}$.

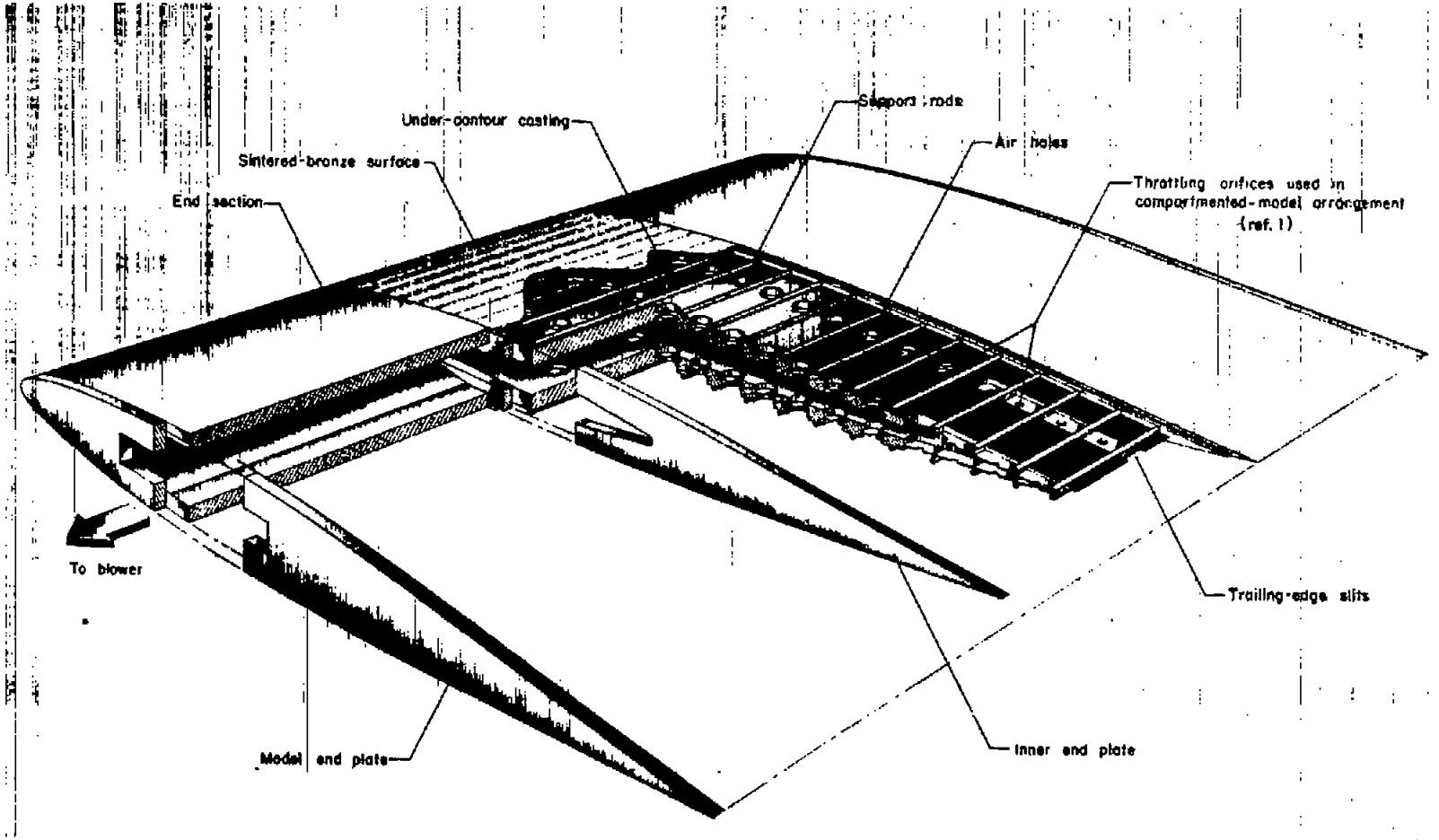

Figure 2.- Construction of NACA 64A010 area-suction airfoil model.

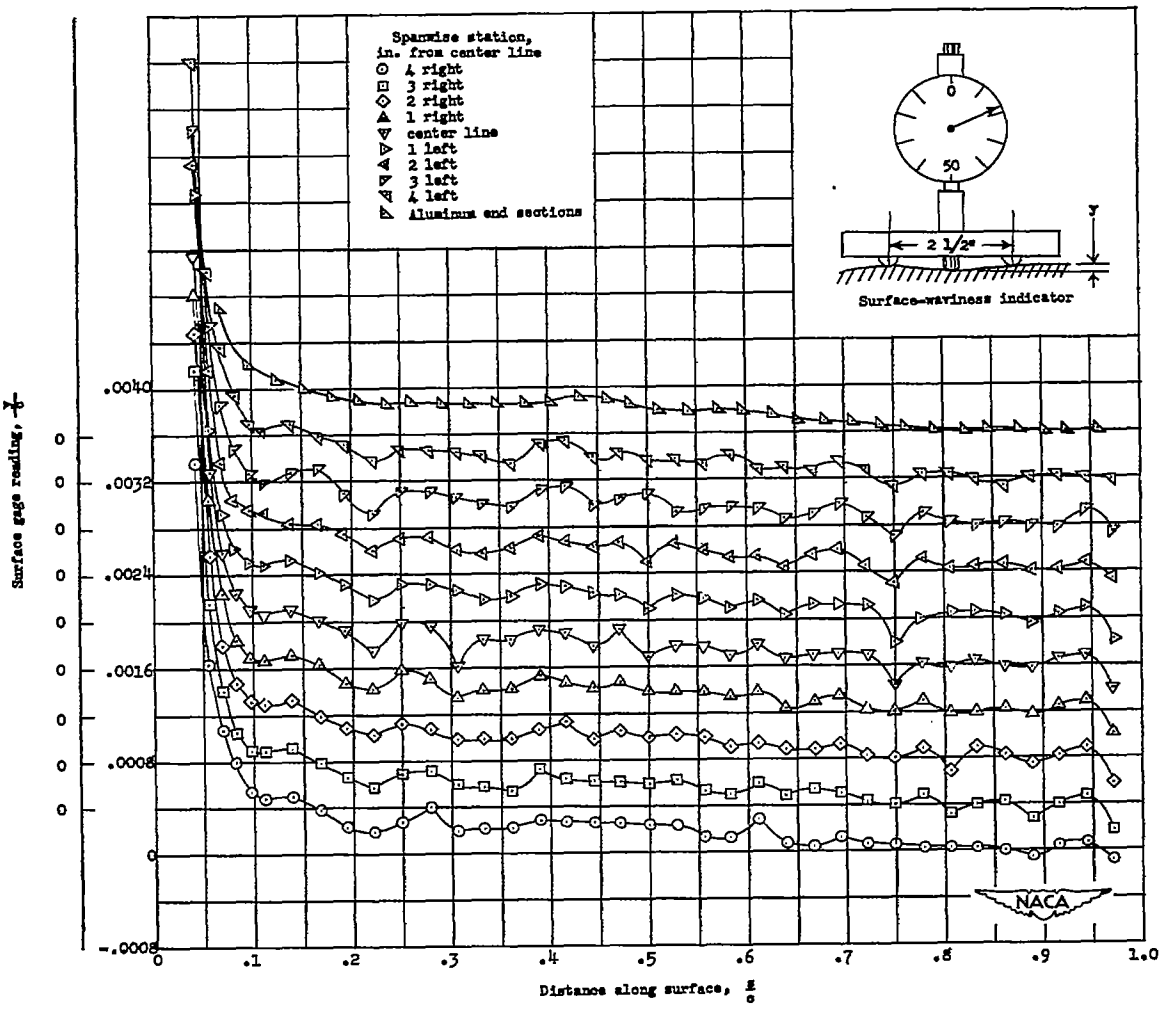

(a) Upper surface.

Figure 3.- Chordwise surface waviness surveys for various spanwise positions across porous-bronze NACA 64A010 airfoil model.

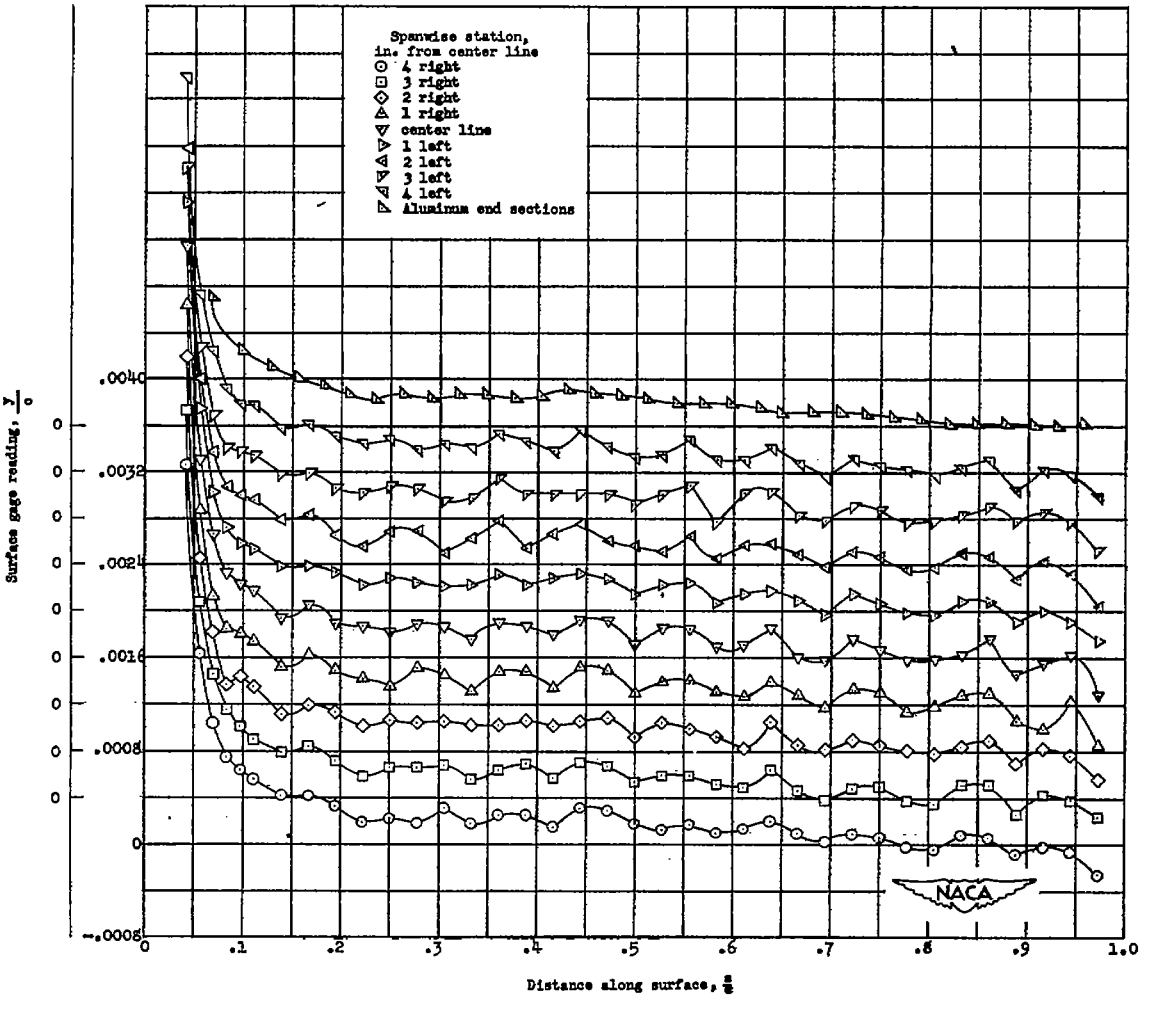

(b) Lower surface.

Figure 3.- Concluded.

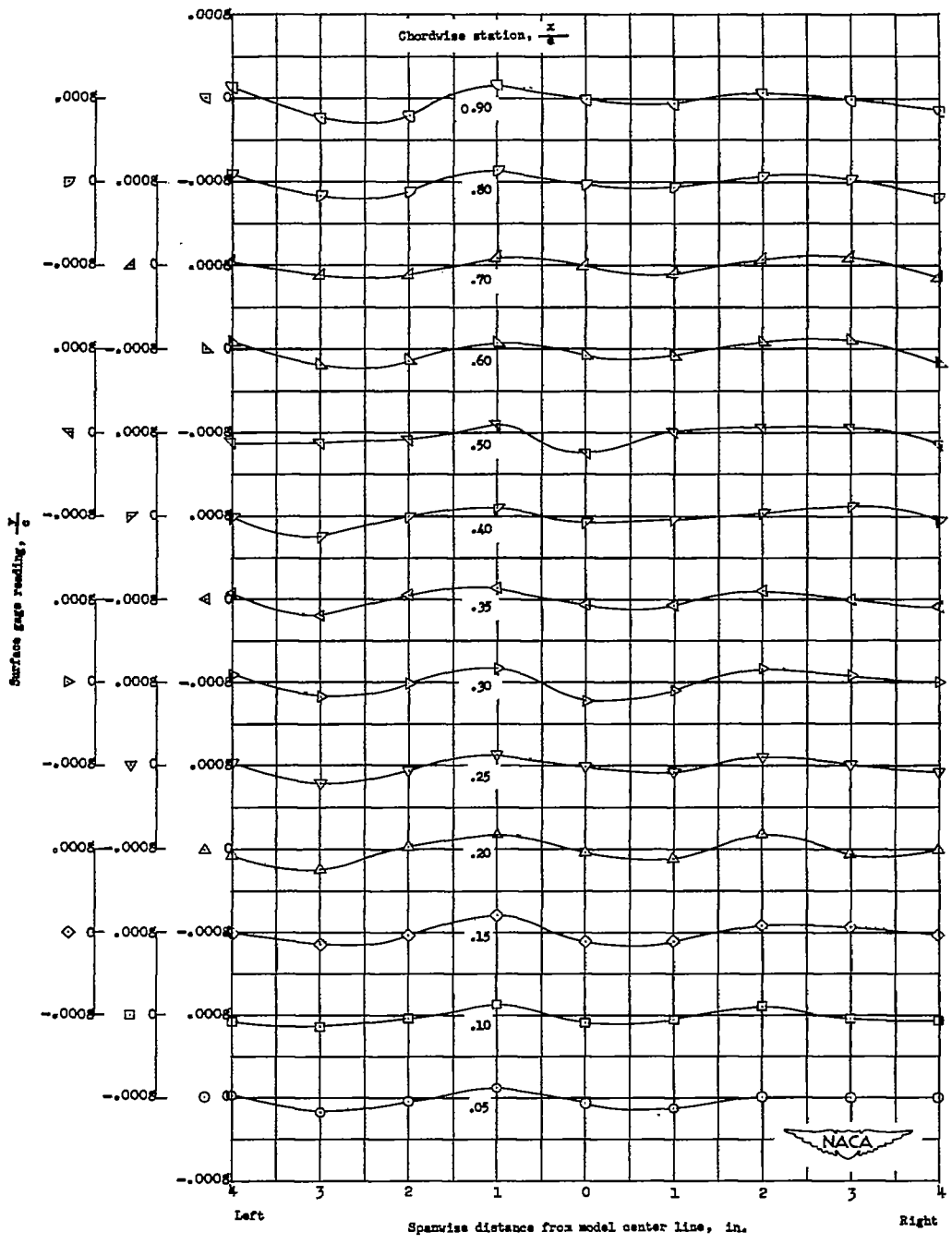

(a) Upper surface.

Figure 4.- Spanwise surface waviness surveys for various chordwise stations across porous-bronze NACA 64A010 airfoil model.

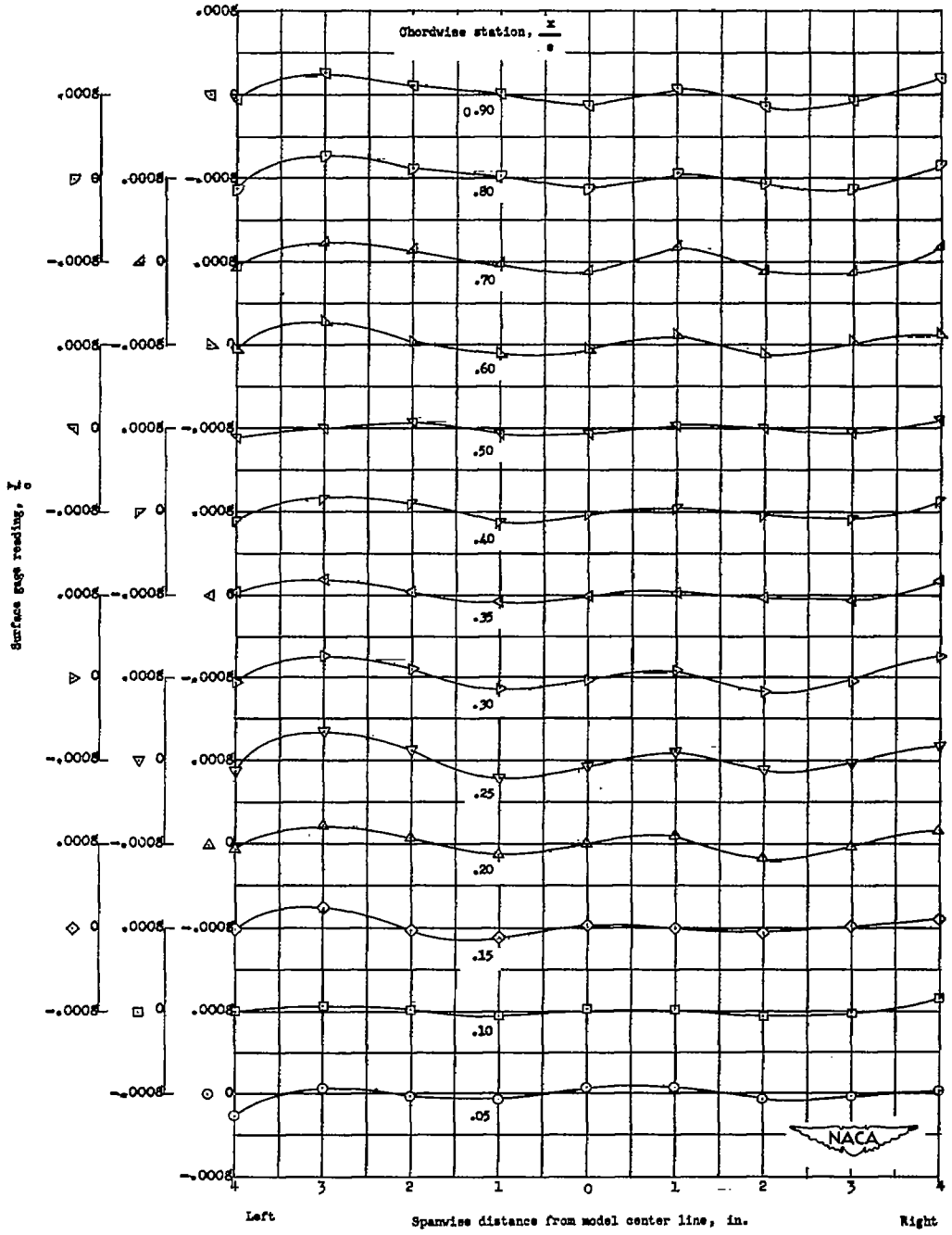

(b) Lower surface.

Figure 4.- Concluded.

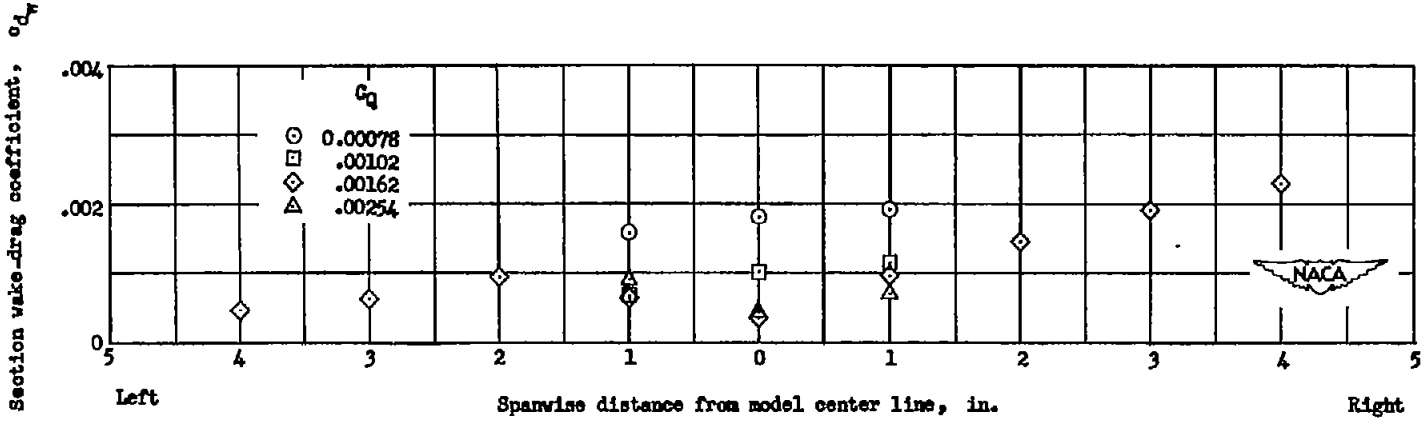

Figure 5.- Spanwise variation of section wake-drag coefficient for porous-bronze NACA 64A010 airfoil model for various suction-flow coefficients. $R = 6 \times 10^6$; $\alpha = 0^\circ$.

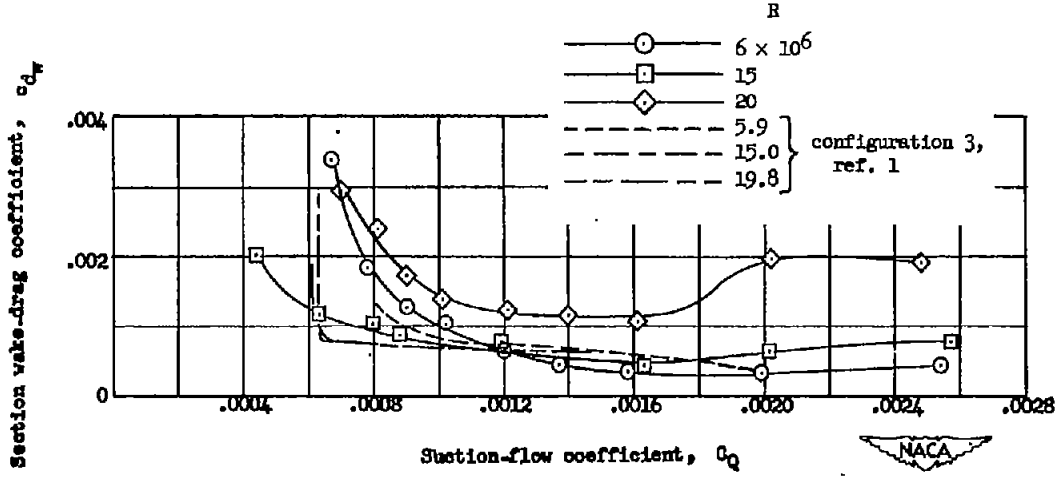

Figure 6.- Variation of section wake-drag coefficient at model center line with suction-flow coefficient for porous-bronze NACA 64A010 airfoil model. $\alpha = 0^\circ$.

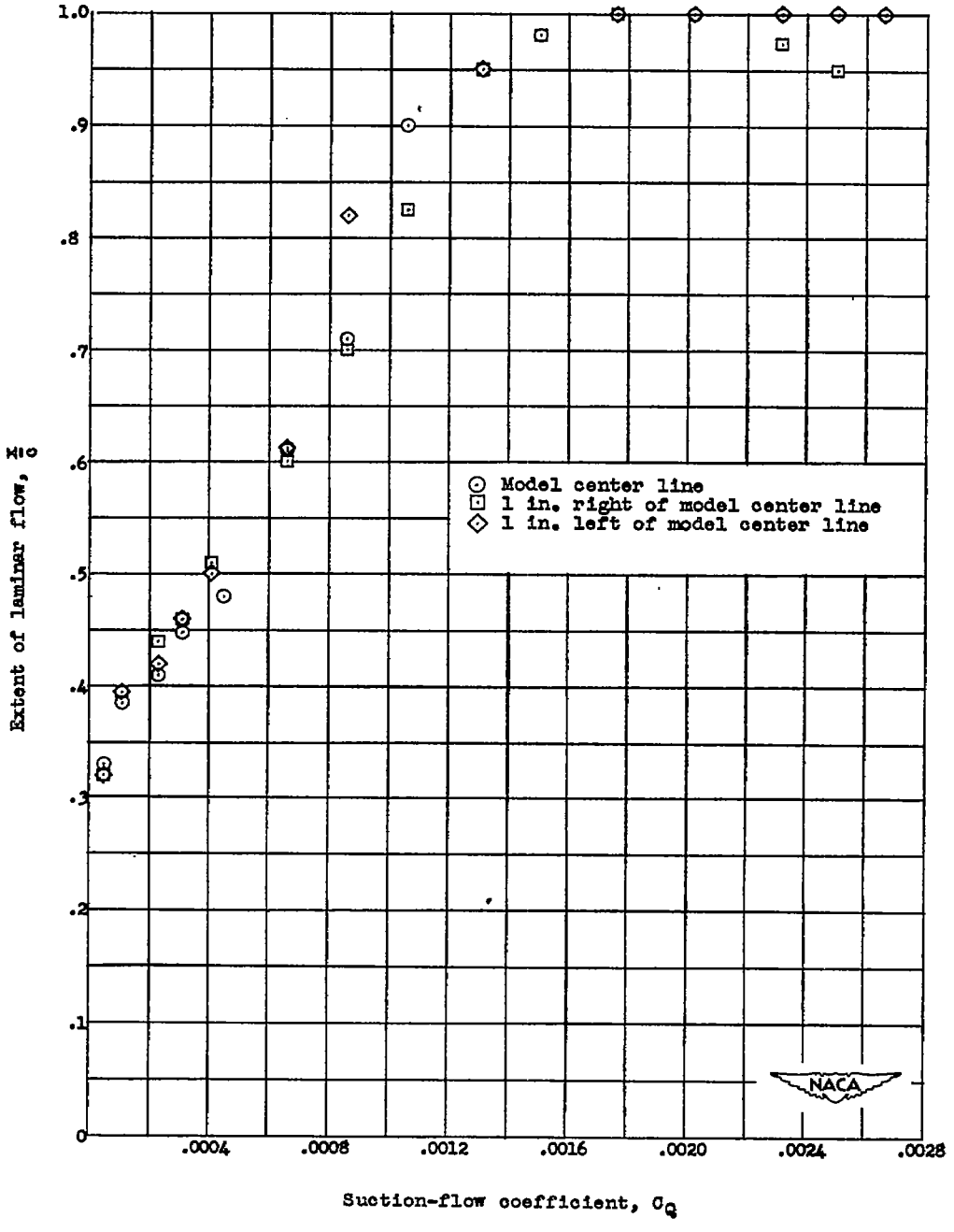

Figure 7.- Extent of laminar flow at three spanwise positions on the upper surface of the porous-bronze NACA 64A010 airfoil model for various suction-flow coefficients. $R = 6 \times 10^6$; $\alpha = 0^\circ$.

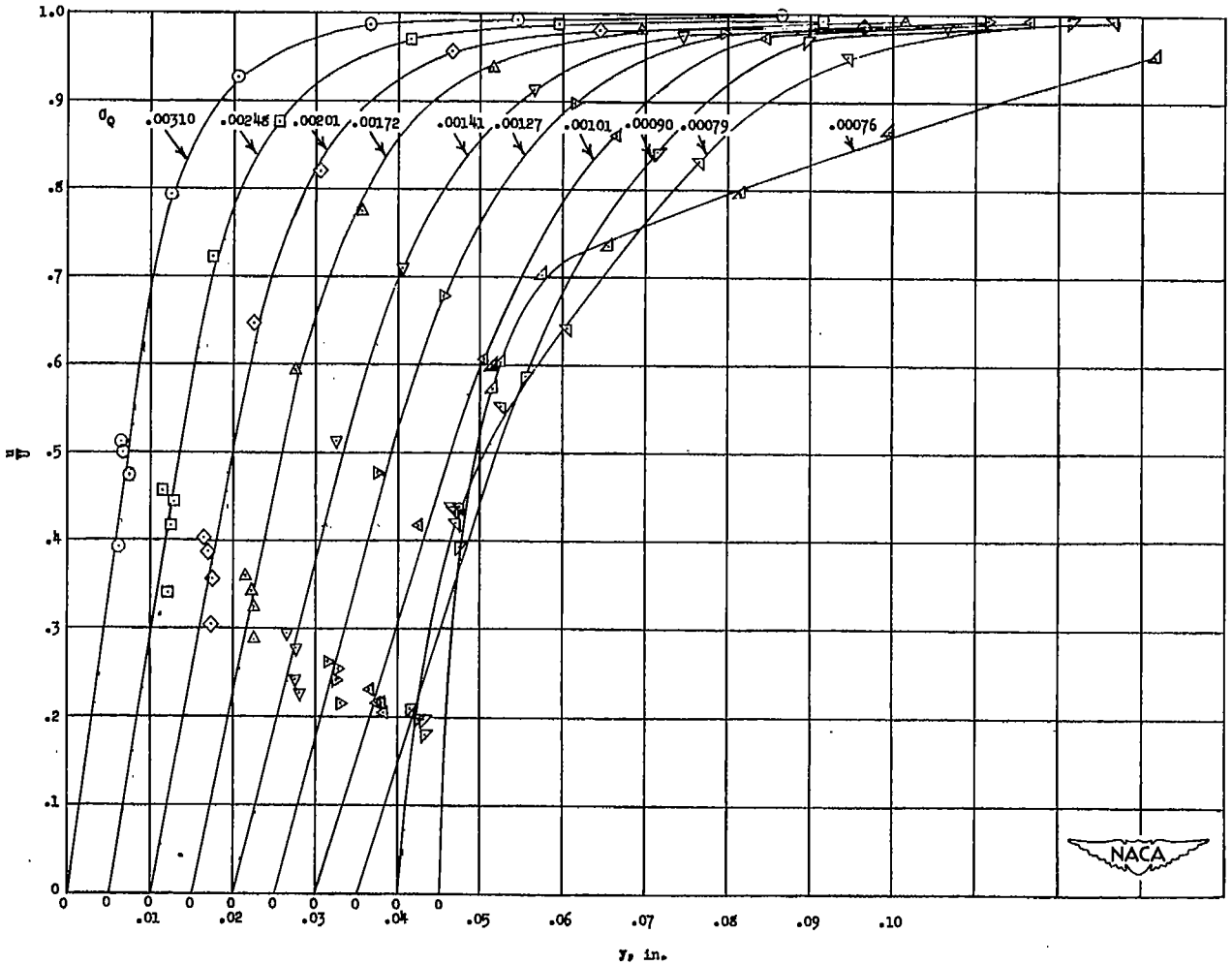

Figure 8.- Boundary-layer profiles measured on the upper surface of the porous-bronze NACA 64A010 airfoil model at $\frac{x}{c} = 0.75$ for a number of suction-flow coefficients. $R = 6 \times 10^6$; $\alpha = 0°$.

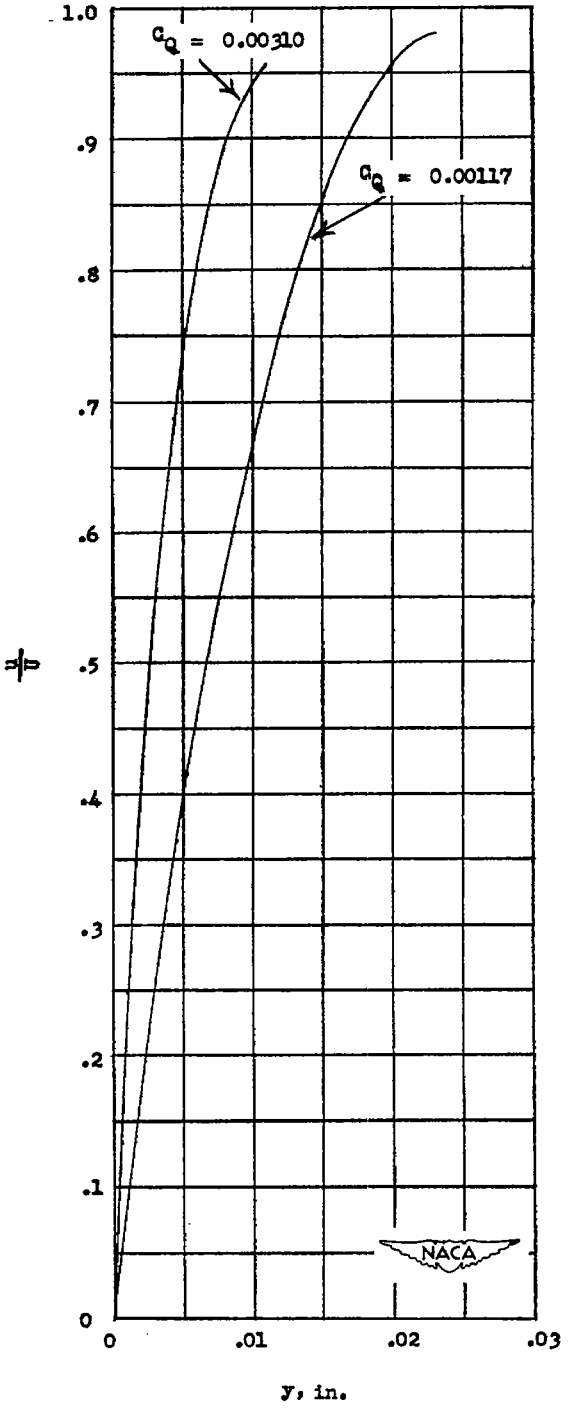

Figure 9.- Boundary-layer profiles at 0.30c calculated for the porous-bronze NACA 64A010 airfoil by the method of reference 5 for two suction-flow coefficients. $R = 6 \times 10^6$; $\alpha = 0^\circ$.

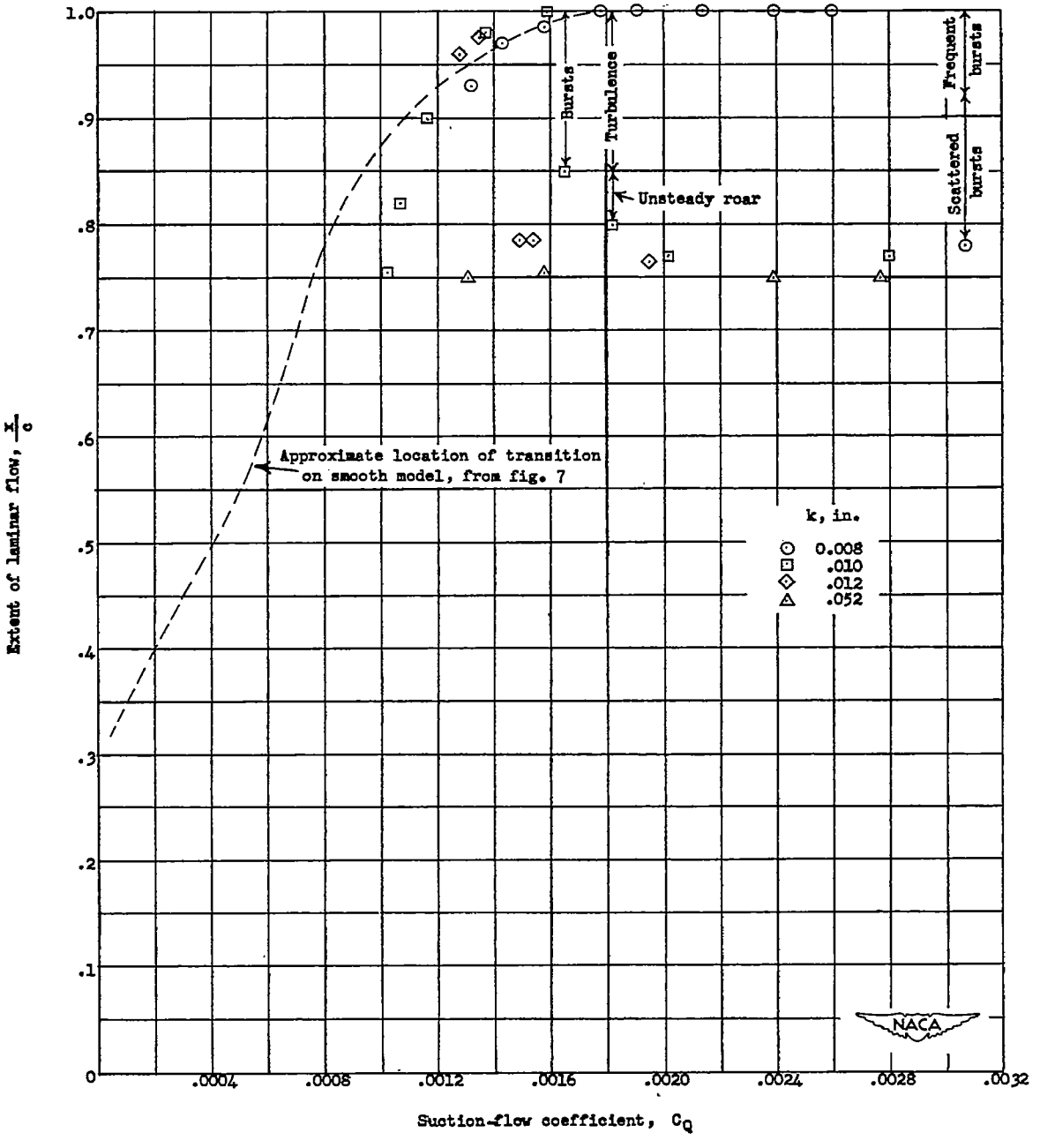

Figure 10.- Extent of laminar flow behind a projection of 0.024-inch diameter, at several projection heights, located 1 inch left of model center line at $\frac{x}{c} = 0.75$ on the upper surface of the porous-bronze NACA 64A010 airfoil model for various suction-flow coefficients. $R = 6 \times 10^6$; $\alpha = 0^\circ$.

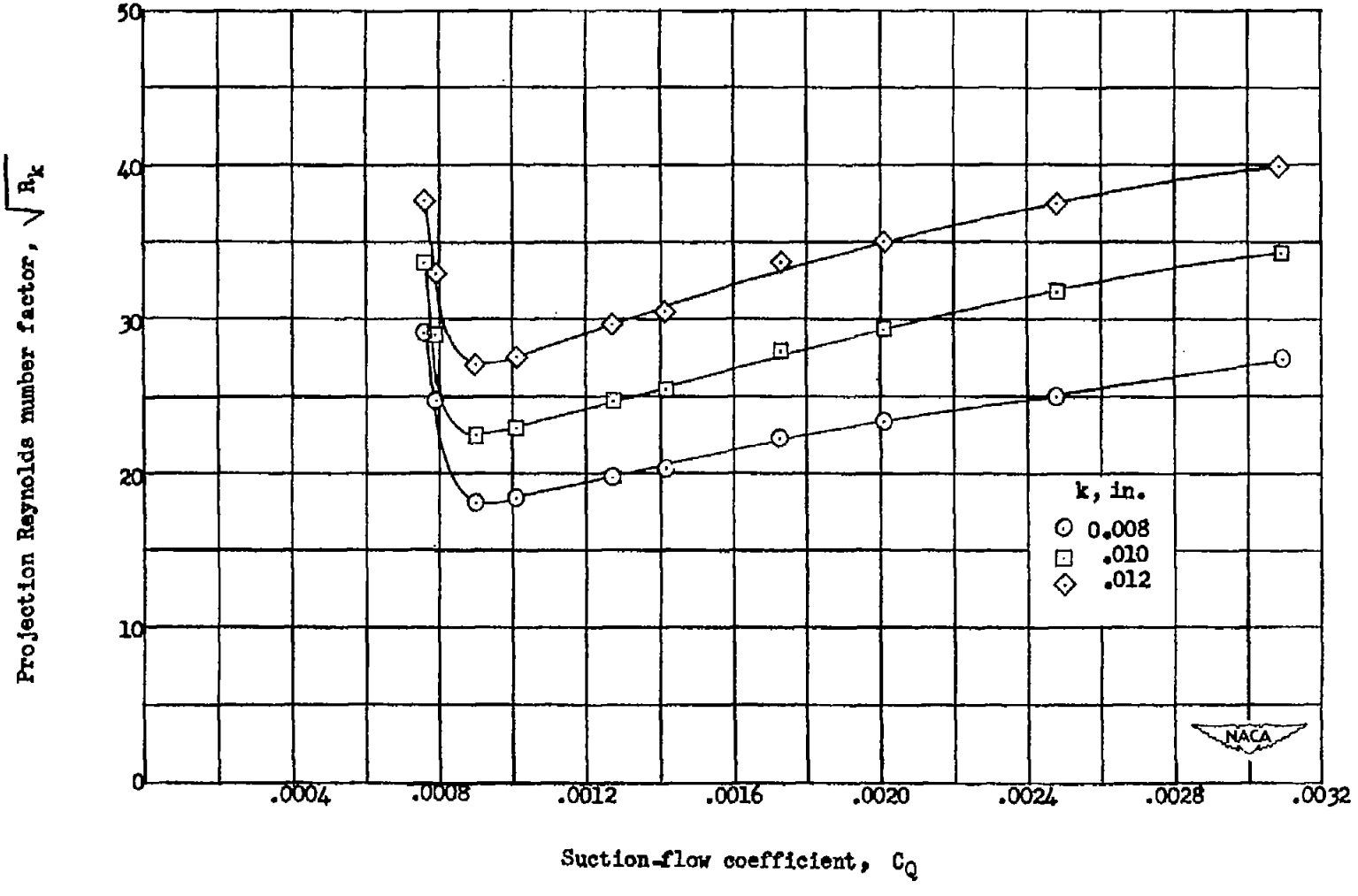

Figure 11.- Variation of projection Reynolds number with suction-flow coefficient for three values of the projection height at 0.75c. $R = 6 \times 10^6$; $\alpha = 0^\circ$.

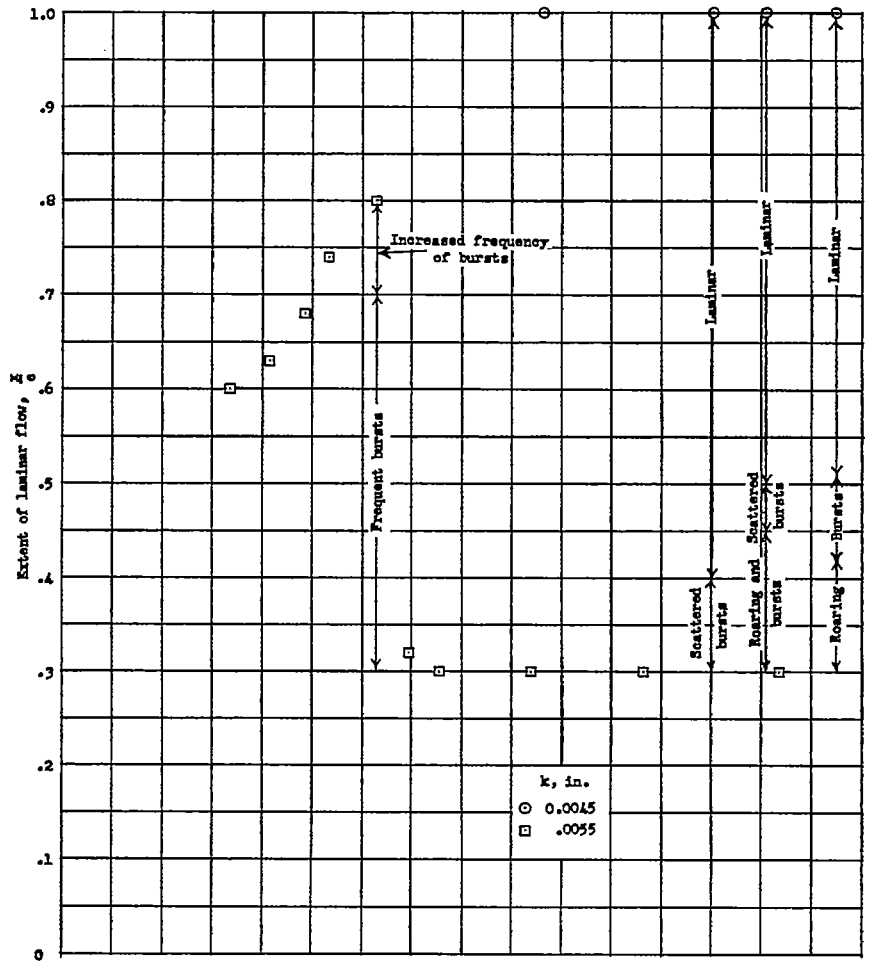

(a) Extent of laminar flow.

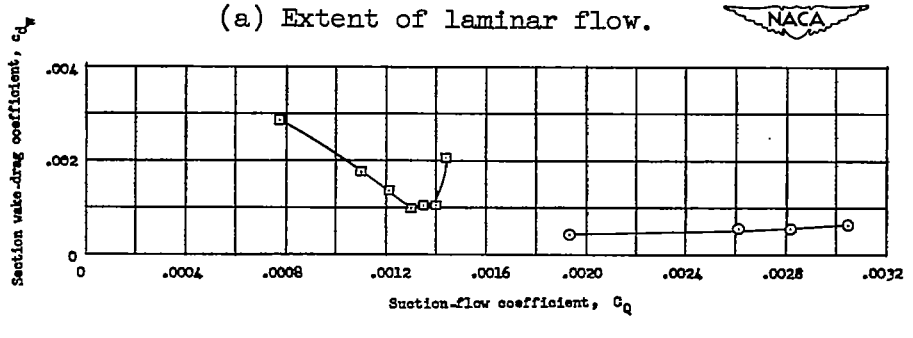

(b) Section wake-drag coefficient.

Figure 12.- Extent of laminar flow and section wake-drag coefficient measured on the porous-bronze NACA 64A010 airfoil model behind a projection of 0.024-inch diameter, at two projection heights, located on model center line at $\frac{x}{c} = 0.30$ on the upper surface for various suction-flow coefficients. $R = 6 \times 10^6$; $\alpha = 0^\circ$.

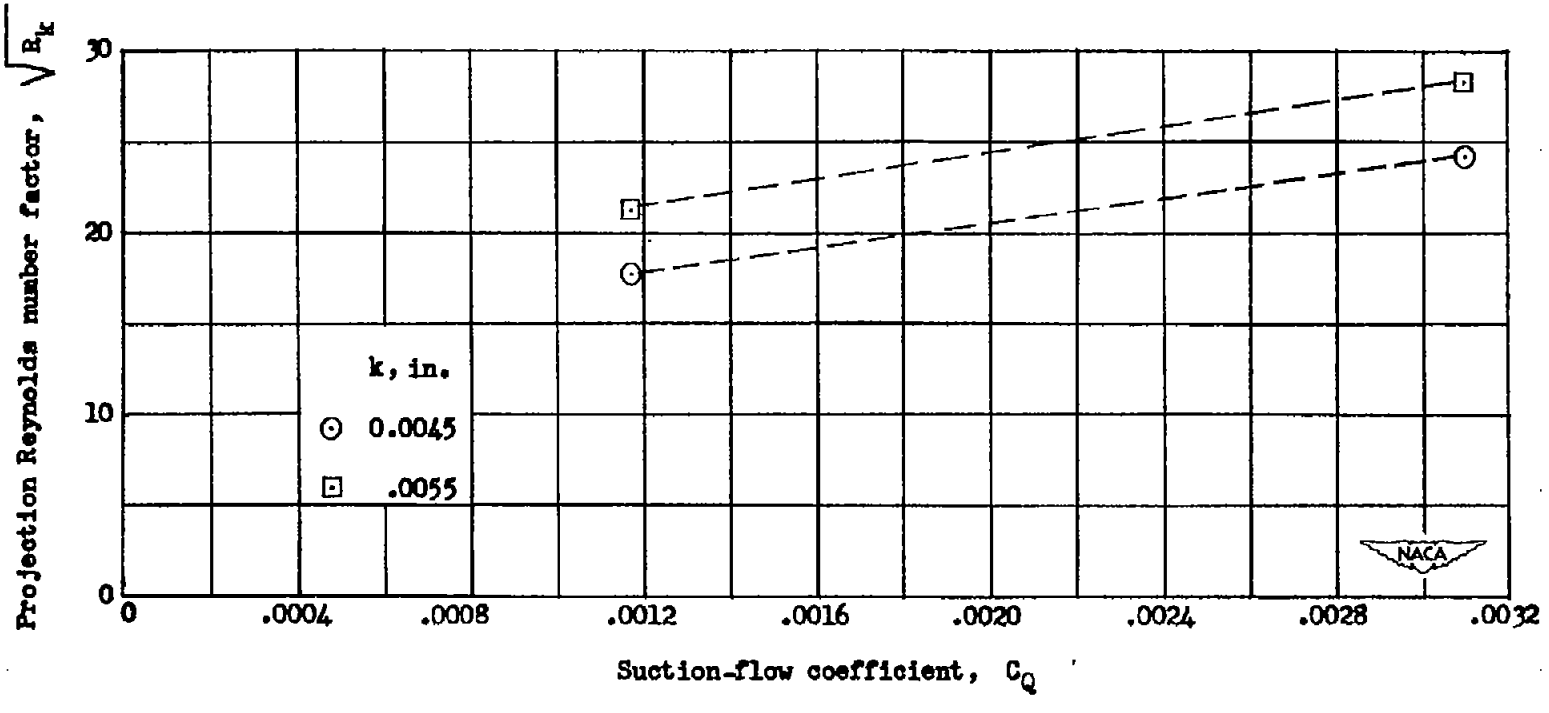

Figure 13.- Variation of projection Reynolds number factor with suction-flow coefficient for two values of the projection height at 0.30c. $R = 6 \times 10^6$; $\alpha = 0^\circ$.

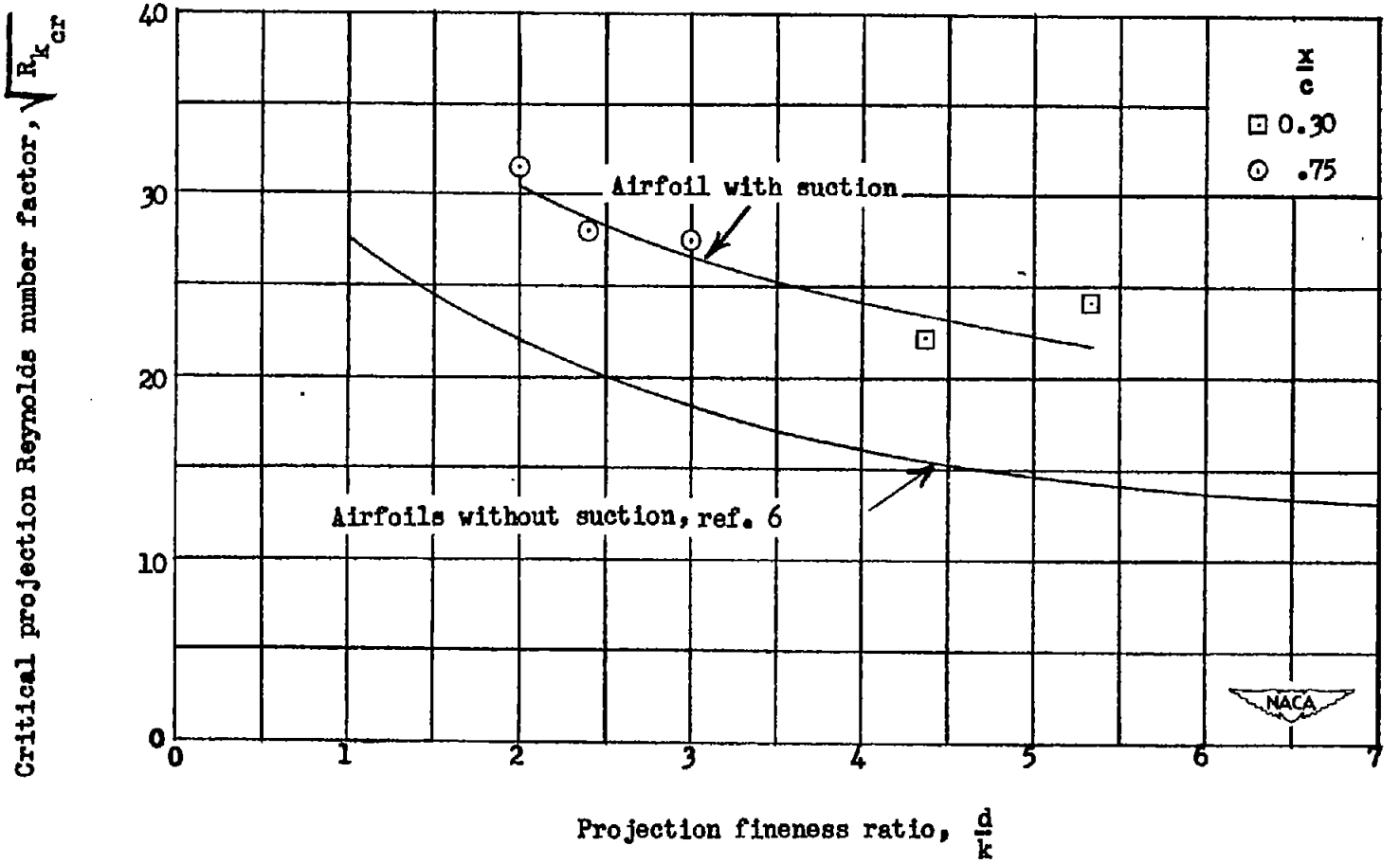

Figure 14.- Variation of critical projection Reynolds number factor with fineness ratio for the porous-bronze NACA 64A010 airfoil model and the airfoils without suction, reference 6.

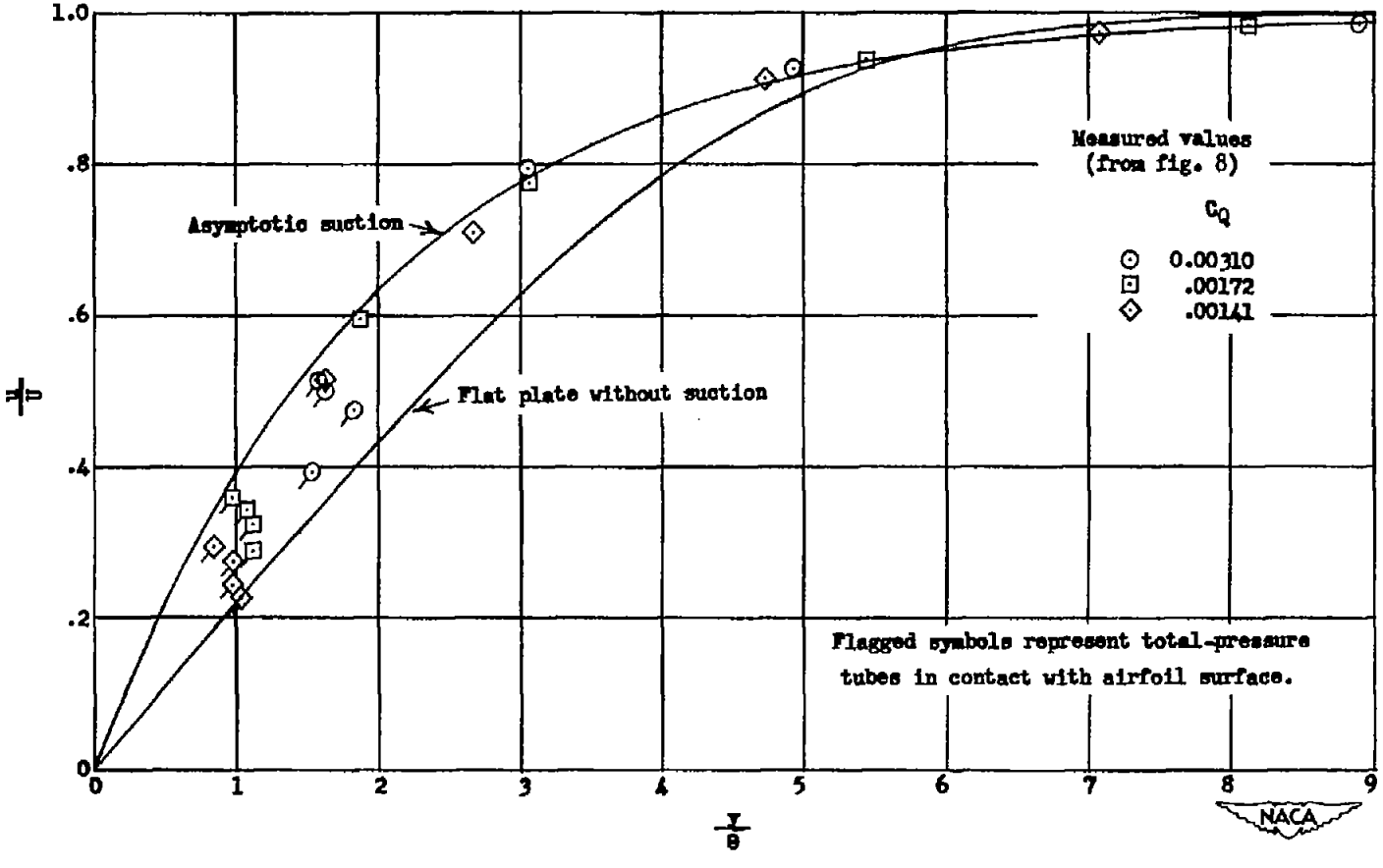

Figure 15.- Comparison of boundary-layer velocities measured on the NACA 64A010 airfoil at 0.75c with the asymptotic suction and the nonsuction flat plate types of boundary-layer velocity profiles.

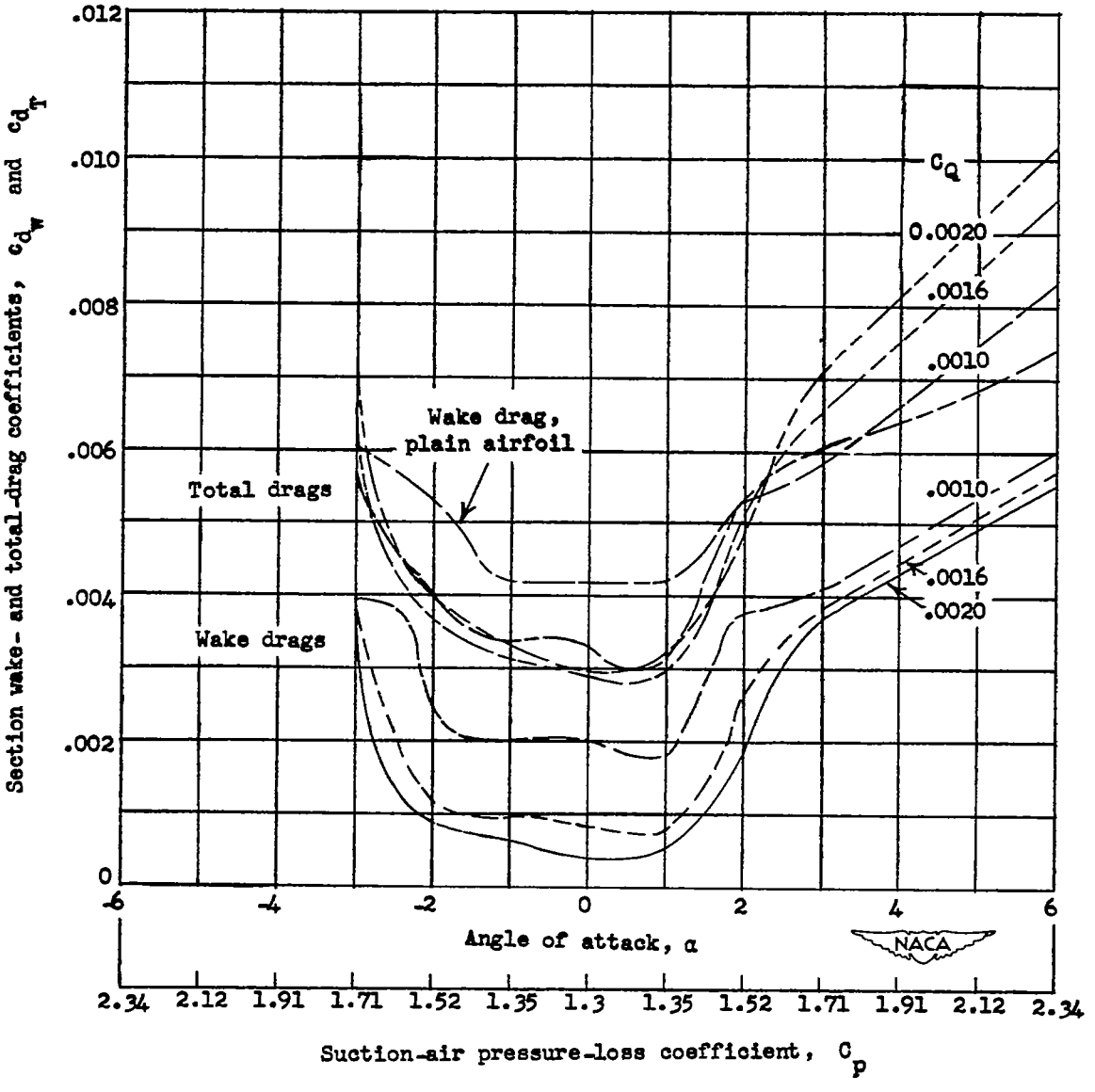

Figure 16.- Variation of section wake-drag and section total-drag coefficients measured at model center line, based on the minimum suction-air pressure-loss coefficient required to prevent outflow, with angle of attack for several suction-flow coefficients for the porous-bronze NACA 64A010 airfoil model. $R = 6 \times 10^6$.